Title

An off/on thrombin activated energy driven molecular machine for sensitive detection of human thrombin via non-enzymatic catalyst recycling amplification

Zhang Zhang[a], Min Mei[a], Juan Yao[b],Ting Ye[a], Jing Quan[a], Jinbo liu[a]*

[a] Department of Laboratory Medicine, The Affiliated Hospital of Southwest Medical University, Luzhou, China

[b] Department of Laboratory Medicine, The Affiliated Traditional Chinese Medicine Hospital of Southwest Medical University, Luzhou, China

*Corresponding author. E-mail: liulab2019@163.com and cqzhangzhang@gmail.com

Table S1 Sequences of the designed oligonucleotides catalyst

Name	Sequences(5′-3′)
Aptamer	Dabcyl-AGTCCGTGGTAGGGCAGGTTGGGGTGACT
Aptamer control	AGTCCGTGCTAGGCCAGGTTGAGGTGACT
Catalyst-FAM	AGTCACCCCAACCTGCCCTACC-FAM
Catalyst	AGTCACCCCAACCTGCCCTACC
Fuel strand	FAM-CCTACGTCTCCAACTAACTTACGGCCCTAGTCACCCCAACCTGC
Signal probe	ROX-CCTACGTCTCCAACTAACTTACGG
Assistant probe	CCCTAGTCACCCCAACCTGC
Linker	GGTAGGGCAGGTTGGGGTGACTAGGGCCGTAAGTTAGTTGGAGACGTAGG-Dabcyl

Note: The matching colour letters represented domains of each strand and underlined letters represented complementary sequences of corresponding domains. FAM, ROX and Dabcyl were fluorescent group and quenching group, respectively.

Table S2 Domain sequences of basic target recycling amplification

Domains	Sequences(5′-3′)	Length(nt)
a	CCTACGTCTCCAACTAACTTACGG	24
b	CCCT	4
c	AGTCACCCCAACCTGC	16
d	CCTACC	6

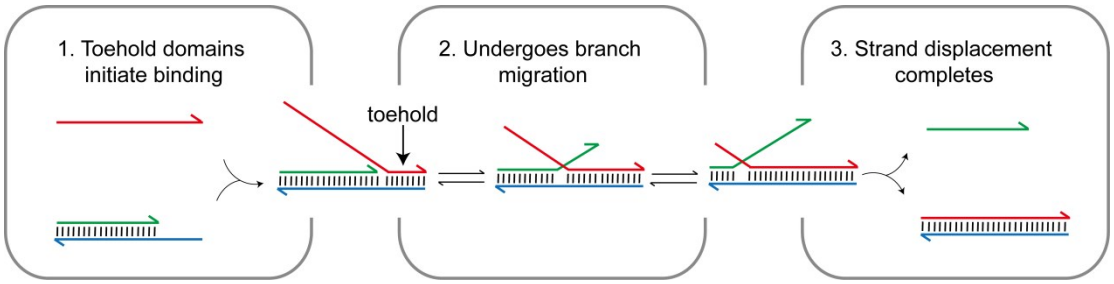

Fig. S1 Scheme illustration of toehold mediated strand displacement reaction

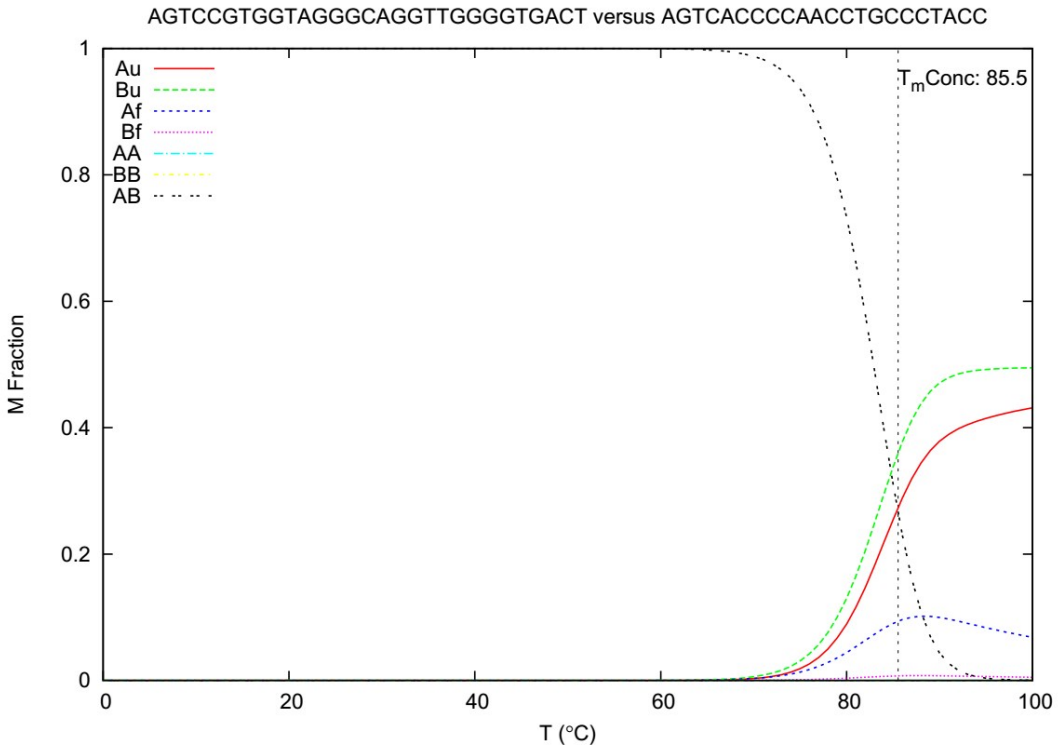

Fig. S2 Mole fractions of aptamer (A) and catalyst (B) are computed as a function of temperature by UNAfold. Au represents unfolded aptamer; Af reprent folded aptamer and AA represent homodimer. The mole fractions of different molecular species were computes using the computed free energies for individual monomer (folded) and dimer (hybridized) species.

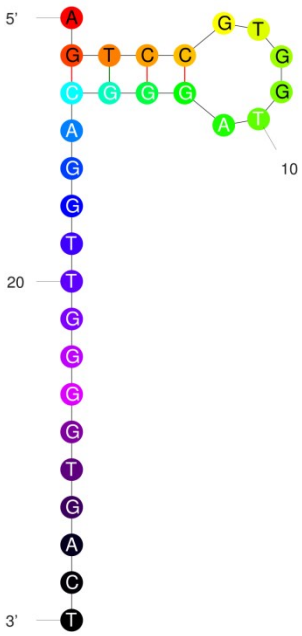

Fig. S3 Predicted secondary structure of thrombin aptamer using UNAfold software online, standard gibbs energy change was calculated to -0.75Kcal/mol

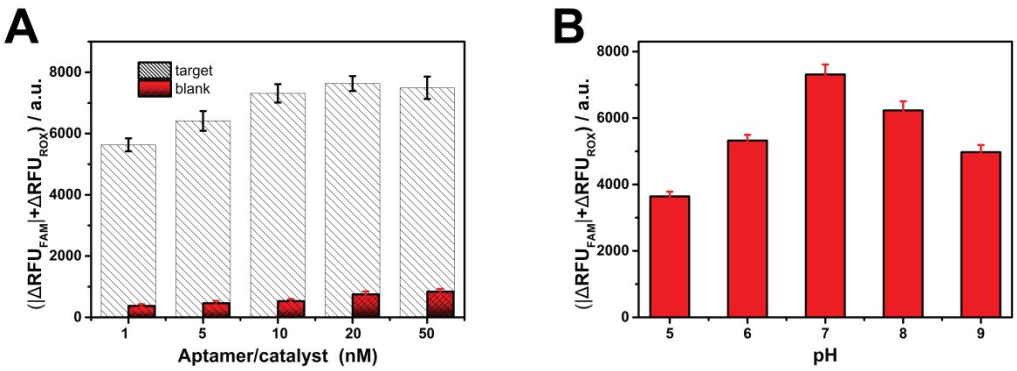

Fig. S4 Optimization of the concentration of substrate (A) and pH (B)

To assess amplification ratio of thrombin in experiments (see Figure S5), different concentrations of ROX labeled signal probe (10 nM, 20 nM, 50 nM, 100 nM, 200 nM) were first analyzed. The linear relationship could be expressed as RFU = 41.80*C (nM). Thus, the signal of ROX in Figure 4A could be converted to ROX concentration. The amplification ratio for different thrombin concentration is then calculated and between 1.4E*2 to 2.9E*7.

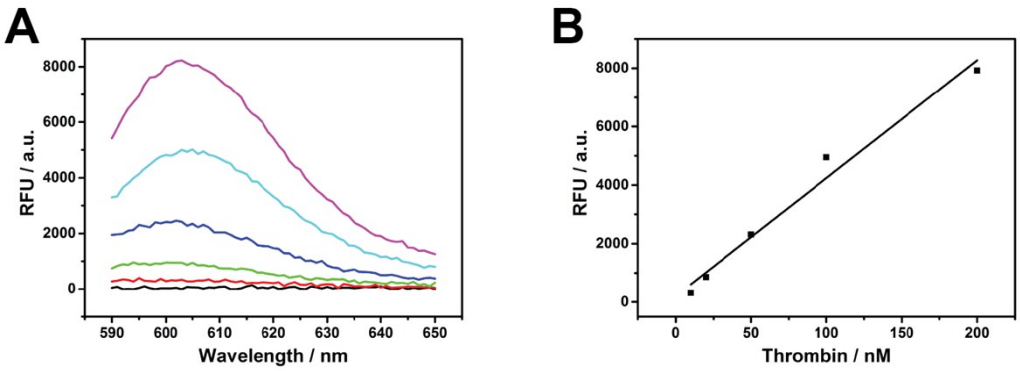

Fig. S5 (A) fluorescence emission spectra of different concentration ROX and (B) corresponding linear relationship

To evaluate the analytical performance of Thrombin ELISA kit (Biovision, USA), Various concentrations of Thrombin (20, 10, 5, 2.5, 1.25, 0.625, 0.313, 0 ng/ml) were analysed using standard protocol. The standard curve can be plotted as the relative OD 450 of each standard solution vs. the respective concentration of the standard solution. The absorbance at 450 nm has a good linear relationship between 20 to 0.625 ng/mL (corresponding to 540 to 17 pM).

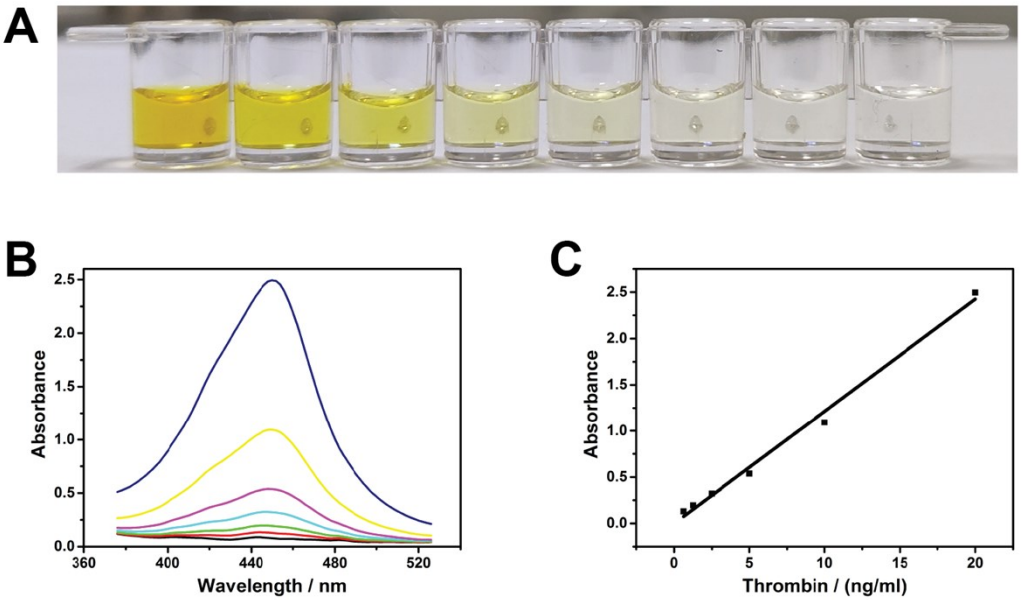

Fig. S6 (A) Photographs of ELISA results for thrombin detection with the bare eyes. (B) Corresponding plasmon absorption spectra for different thrombin concentrations. (C) the liner range (0.625 to 20 ng/mL.) between the absorption intensity at 450 nm and thrombin.

Table S3 Thermodynamic parameters evaluated by UNAfold

Name	Complementary length	Temperature (K)	ΔH° (Kcal/mol)	ΔS° (cal/mol)	ΔG° (Kcal/mol)
Aptamer/Catalyst	22	310.15	-174.1	-462.8	-30.6
Linker/Signal probe	24	310.15	-199.8	-545.3	-30.7
Linker/Assistant probe	20	310.15	-159.1	-424.3	-27.5
Linker/Catalyst	22	310.15	-169.9	-449.7	-30.4
Linker/Fuel strand	44	310.15	-357.3	-957.0	-60.5

Table S4 Comparison of different methods for thrombin detection

Technology	Amplification	Limit-of detection	Dynamic range	Easy Procedure (One-step)	Reference
Electrochemical aptasensor	PANI-MWCNTs	0.08 pM	0.1 pM to 4 nM	No	1
Colorimetric assay	cationic polythiophene	4 pM	0.01 nM to 0.10 nM	Yes	2
Fluorescence biosensing	Au nanoclusters and MnO_2 sheets	0.1 nM	0.2 nM to 20 nM	Yes	3
Fluorescence biosensing	DNAzyme recycling amplification	6.9 pM	0.01 nM to 50 nM	Yes	4
Electrochemiluminescence	PDANS@Ag/C-dots	0.35 fM	1 fM to5 nM	No	5
Surface-Enhanced Raman Scattering	DNAzyme assistant DNA recycling and rolling circle amplification	2.3 fM	10 fM to 10 nM	No	6
ELISA	HRP	8.5 pM	17 pM to 540 pM	No	7
Fluorescence biosensing	DNA molecular machine	0.45 fM	1 fM to 10 nM	Yes	This work

Table S5 Recovery tests of thrombin in human serum samples

Sample	Added (fM)	Measured (fM)	Recovery (%)	RSD (%, n = 3)
1	10	9.73	97.3	3.63
2	100	102.53	102.5	4.73
3	1000	987.53	98.7	3.86

References

1. Su Z, Xu X, Xu H, et al. Amperometric thrombin aptasensor using a glassy carbon electrode modified with polyaniline and multiwalled carbon nanotubes tethered with a thiolated aptamer[J]. Microchimica Acta, 2017, 184(6): 1677-1682.

2. Liu M, Li J, Li B. A colorimetric aptamer biosensor based on cationic polythiophene derivative as peroxidase mimetics for the ultrasensitive detection of thrombin[J]. Talanta, 2017, 175: 224-228.

3. Wang H B, Li Y, Bai H Y, et al. DNA-templated Au nanoclusters and MnO2 sheets: a label-free and universal fluorescence biosensing platform[J]. Sensors and Actuators B: Chemical, 2018, 259: 204-210.

4. Li J, Wang S, Jiang B, et al. Target-induced structure switching of aptamers facilitates strand displacement for DNAzyme recycling

amplification detection of thrombin in human serum[J]. Analyst, 2019, 144(7): 2430-2435.
5. Liu Y, Zhao Y, Fan Q, et al. Aptamer based electrochemiluminescent thrombin assay using carbon dots anchored onto silver-decorated polydopamine nanospheres[J]. Microchimica Acta, 2018, 185(2): 85.
6. Gao F, Du L, Tang D, et al. A cascade signal amplification strategy for surface enhanced Raman spectroscopy detection of thrombin based on DNAzyme assistant DNA recycling and rolling circle amplification[J]. Biosensors and Bioelectronics, 2015, 66: 423-430.
7. https://www.biovision.com/